Impedance Control Strategies for Enhancing Sloped and Level Walking Capabilities for Individuals with Transfemoral Amputation Using a Powered Multi-Joint Prosthesis

*Krishan Bhakta, MS *; Jonathan Camargo, MS *†; Pratik Kunapuli, BS‡; Lee Childers, PhD, CP §‖; Aaron Young, PhD*†*

ABSTRACT Introduction: Powered prostheses are a promising new technology that may help people with lower-limb loss improve their ability to perform locomotion tasks. Developing active prostheses requires robust design methodologies and intelligent controllers to appropriately provide assistance to the user for varied tasks in different environments. The purpose of this study was to validate an impedance control strategy for a powered knee and ankle prosthesis using an embedded sensor suite of encoders and a six-axis load cell that would aid an individual in performing common locomotion tasks, such as level walking and ascending/descending slopes. Materials and Methods: Three amputees walked on a treadmill and four amputees walked on a ramp circuit to test whether a dual powered knee and ankle prosthesis could generate appropriate device joint kinematics across users. Results: Investigators found that tuning 2–3 subject-specific parameters per ambulation mode was necessary to render individualized assistance. Furthermore, the kinematic profiles demonstrate invariance to walking speeds ranging from 0.63 to 1.07 m/s and incline/decline angles ranging from 7.8° to 14°. Conclusion: This work presents a strategy that requires minimal tuning for a powered knee & ankle prosthesis that scales across a nominal range of both walking speeds and ramp slopes.

INTRODUCTION

People with a transfemoral amputation using traditional passive prostheses ambulate with a variety of walking abnormalities. These individuals experience asymmetric loading between the intact and residual limb joints.[1] Certain individuals also suffer from chronic leg and back pain.[2] A goal in transfemoral prosthesis design has been to restore the lost function from both the knee and ankle joints. However, the vast majority of currently available prosthetic feet (e.g., Össur Vari-flex foot) and knees (e.g., Ottobock's C-Leg and Össur's Rheo Knee) are passive (i.e., provides no net power).[3,4] The use of resulting compensatory strategies to walk that include greater moments on the intact limb may lead to joint degradation, pain, and osteoarthritis.[1,5–7] Development of actively controlled powered prosthetic joints may reduce these post-amputation compensatory strategies.[8–10]

Prosthetic hardware has been designed to alleviate and provide powered assistance to the user under different locomotion tasks.[11–17] However, creating a controller that can coordinate knee and ankle joints to provide the appropriate amount of assistance/resistance has been challenging.[18–20] An additional consideration is ensuring that two independently powered joints can be controlled in unison to have efficient and stable dynamics. Various controllers have also been tested to improve functionality and robustness of these devices during dynamic movements.[14,21–26] Impedance controllers implemented on powered transfemoral prostheses were among the first controllers to provide stable and coordinated user interaction with the environment.[27,28] Using an impedance controller paired with a finite-state machine, which identifies critical points in the gait cycle, allows for the easy configuration of parameters to adjust gait for different tasks.[8]

Different research groups have developed their own prosthetic devices to help individuals with amputation, showing mechanical improvements over time; however, creating robust and smart controllers for dynamic activities is still underexplored.[13,16,27] To achieve lower cost and weight requirements, some research groups have focused on single-joint prostheses and semi-active prostheses to improve common walking tasks without the need of bulky power sources.[16,29] A challenge with powered multi-joint prosthetic systems has always been the integration of a sensor suite with a control system that can recognize different tasks and environments the person is walking in and responding accordingly. We have developed a powered knee-ankle prosthesis and control testbed by starting with a well-defined task (e.g., steady-state walking) where the intent of the user is known before progressing to more complex tasks (overground walking, ramps, stairs, etc.). In this development

*Woodruff School of Mechanical Engineering, College of Engineering, Georgia Institute of Technology, Atlanta, GA USA
†Institute for Robotics and Intelligent Machines, Georgia Institute of Technology, Atlanta, GA USA
‡School of Electrical and Computer Engineering, College of Engineering, Georgia Institute of Technology, Atlanta, GA USA
§Center for the Intrepid, Department of Rehabilitation Medicine, Brooke Army Medical Center, JBSA Ft. Sam Houston, TX, USA
‖Extremity Trauma and Amputation Center of Excellence, JBSA Ft. Sam Houston, TX, USA
Corresponding author: walter.l.childers.civ@mail.mil
doi:10.1093/milmed/usz229

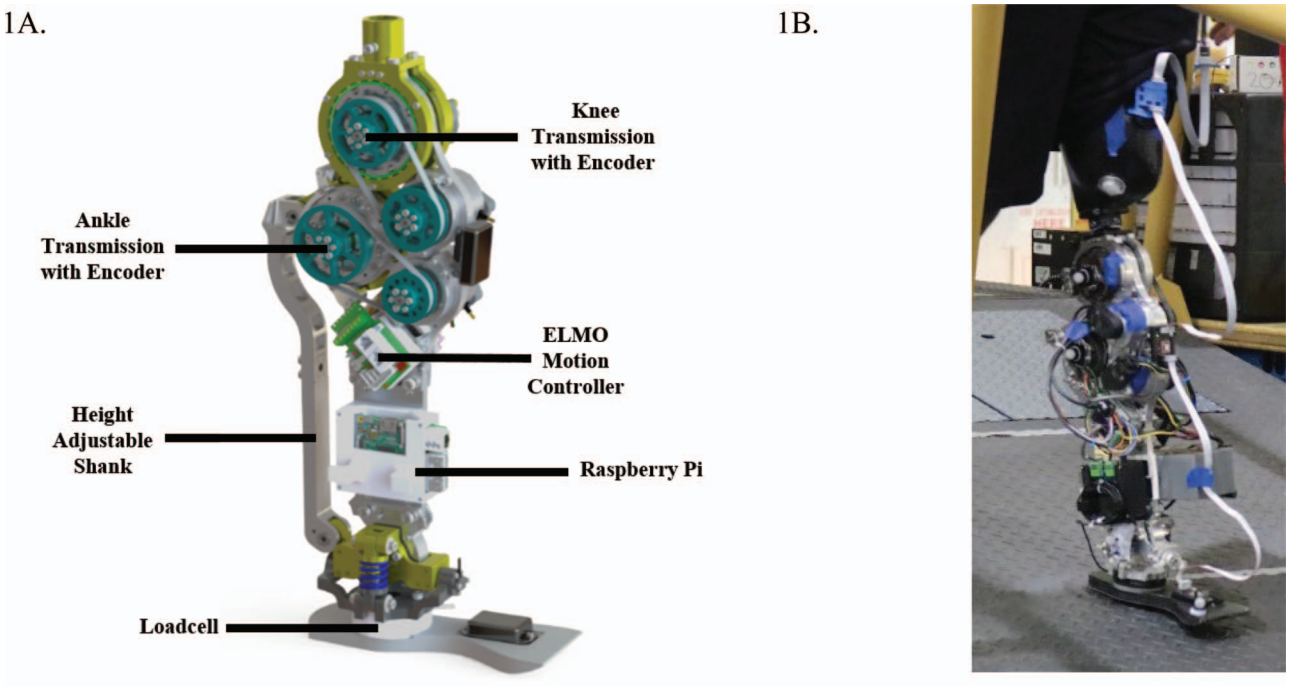

FIGURE 1. (A) Features of the device including: knee transmission with encoder (top right), ankle transmission with encoder (top left), ELMO motion controller (middle right), microprocessor (middle right), height-adjustable shank (middle left), and 6-DOF load cell (bottom left). (B) User walking with a prosthetic device on a ramp.

project, we defined success as a prosthesis that could (1) correctly recognize the different phases of gait, (2) tune joint impedance to scale across a range of gait speeds/inclination angles, and (3) generate knee and ankle kinematics similar to individuals without transfemoral amputation.

METHODS

Powered Prosthetic Device

The investigators developed a new iteration of a previous device,[30] from a collaboration between the Exoskeleton and Prosthetic Intelligent Controls lab at Georgia Institute of Technology and the Advanced Mechanical Bipedal Experimental Robotics Lab at California Institute of Technology (Fig. 1). The device has one actuated degree-of-freedom (DOF) at the knee joint in the sagittal plane, and two DOFs at the ankle—a powered DOF in the sagittal plane and a passive DOF in the frontal plane. The device is approximately 7.5 kg including the battery, which is similar to the missing biological limb mass (i.e., 13% of body weight),[31] and has adjustable build heights of 46–63 cm to accommodate different residual limb lengths. Both knee and ankle joints are actively controlled using two 206 W brushless DC motors (MOOG BN23), which are capable of achieving approximately 1 N-m peak torque. To mimic human biological torque capabilities, the device utilizes a gear transmission ratio of 1:175 at the ankle joint and 1:120 at the knee joint. The gearbox consists of a harmonic drive (model CSG-17-100-2UH-LW, Harmonic Drive, Peabody, MA) that reaches a 1:100 reduction and a variable pulley-belt system that produces the remaining gear reductions for both joints. The mechanical properties of each joint have an estimated efficiency of 70% (Supplementary Table S1).[30] Our powered multi-joint prosthesis is unique because it allows for closed-loop torque control with the series-elastic actuators, passive frontal plane DOF, and serves as a good controls testbed for implementing different controllers.

A raspberry pi 3 model B microprocessor (4×ARM Cortex-A53, 1.2 GHz) acts as the hardware–software interface platform, where all signal data is measured and logged. Both knee and ankle joints feature an incremental encoder (US Digital E5) concentrically placed in series with the motor, which measures both joint angle and velocity and is controlled through a motion controller (gold solo whistle controller, model G-SOLWHI20/100SE, ELMO Motion Control Technologies, Petah Tikva, Israel) over Controller Area Network (CAN) bus. The raspberry pi also incorporates a 6-DOF load cell (SRI M3714C2) to measure ground reaction forces over CAN bus. The whole system is powered through a 10-cell (37 V), 3600 mAh Li-Po battery (Venom Power) and a portable power bank for the Raspberry Pi (Fig. 1). Device controls are programmed in C++ packages that operate on the robot operating system platform. An accompanying graphical user interface capable of relaying live signals was developed using Python packages.

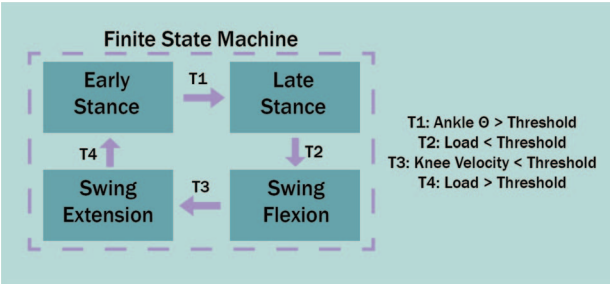

FIGURE 2. Demonstrates the finite state machine for a single ambulation mode, where the gait cycle is discretized into four states. T1 threshold was just a constant that had to be passed in order to transition. T2 and T4 were constants that represented % body weight of the user. T3 threshold was a constant multiplied by the peak knee velocity, where the constant was between 0 and 1. Each state had a unique set of virtual stiffness and damping (impedance) parameters for both the knee and ankle.

Control System

The investigators implemented a hierarchical control paradigm, featuring a high-, a mid-, and a low-level controller. The high-level controller uses machine learning and sensor fusion techniques to estimate user intent, environmental features and user state in real-time, and dynamically adapt to real-world environments. The low-level controller interfaces with the mid-level controller to ensure that the desired torque is actuated at each joint via series-elastic actuators and closed-loop feedback control. Both the high- and the low-level controllers are not a focus of this manuscript but can be seen in previous literature.[20,32–34]

The prosthetic device utilized a mid-level impedance-based controller paired with a finite state machine that allowed for dynamic interaction between the user and environment.[14,27,35,36] Thus, unlike a pure kinematic trajectory control approach, the system does not control user kinematics directly. The gait cycle is broken into discrete states (early/mid-stance, late stance, swing-phase flexion, and swing-phase extension), and in each state, a pair of impedance control laws govern the torque at the knee and ankle joints (Fig. 2).

The impedance controller models each joint as a virtual spring-damper system, where virtual spring stiffness (k), spring equilibrium angle (θ_e), and damping coefficient (b) can be adjusted to modify the desired torque of the joint (Eqn. 1).

$$\tau_{\text{desired}} = -k\,(\theta - \theta_e) - b\dot{\theta} \tag{1}$$

Transitions between states were carried out via a state machine that primarily used sets of thresholds based on mechanical sensors (i.e., encoders and 6-DOF load cell). These thresholds were adjustable by the experimenters to accommodate different gait patterns. The pairing of the finite state machine and the impedance controller allowed for power generation at key moments in the gait cycle, such as powered plantar flexion during push-off, powered knee flexion swing initiation, powered knee swing extension assistance, and stiffening of the knee and ankle for braking during early- to mid-stance. Additionally, three modes of ambulation were implemented (level-ground walking, ramp ascent (RA), and ramp descent (RD)), each with a unique finite state machine. The investigators implemented scaling equations into the finite state machine to smooth transitions between states and reduce the number of independently tuned parameters. The rationale for implementing these equations can be found in previous work.[8] Before any tuning was performed, an input of the user's body mass was required to use some of the following equations. The first scaling equation (Eqn. 2) modulated the ankle stiffness as a function of ankle angle and body weight based on previous studies that have rigorously determined ankle impedance as a function of the ankle in able-bodied subjects.[37] The second equation (Eqn. 3) scaled an impedance parameter from a specified starting value (p_{start}) to a specified final value (p_{final}) as a function of the vertical load on the prosthesis. This equation allowed for smooth transitioning of impedance parameters as the weight was removed from the prosthesis. The last scaling equation (Eqn. 4) altered knee equilibrium angle as a function of the knee angle, which is useful for providing smooth resistance during the ramp decline mode.[8]

$$k_{\text{ankle}} = \text{BM} \times (0.237 \times \theta_{\text{ankle}} + 0.028) \tag{2}$$

$$p = \frac{F_{\text{vertical}}}{\text{BM}} \times (p_{\text{start}} - p_{\text{final}}) + p_{\text{final}} \tag{3}$$

$$\theta_{e,\text{knee}} = C \times \theta_{\text{knee}} \tag{4}$$

Experimental Design

Six individuals (5 male and 1 female) with unilateral transfemoral amputation were recruited and provided informed consent according to the Georgia Institute of Technology Institutional Review Board (Protocol H16351: User-Independent Intent Recognition on a Powered Transfemoral Prosthesis; Supplementary Table S2).

The shank height of the device was adjusted to align the knee center of rotation of the prosthesis with the patient's biological knee center. The device was fitted and aligned by a certified prosthetist and the patient walked in a set of parallel bars over the ground while learning how to utilize powered assistance. Control parameters and prosthetic alignment were tuned and observed during this time to ensure the comfortable transfer of power during walking and minimization of clinical gait deviations. This adjustment period typically took 30–45 minutes per subject. In total, there are 28 parameters that can be adjusted per ambulation mode to modify the gait dynamics. Two experimental protocols were conducted after the initial tuning session, three participants (TF01, TF02, and TF03) performed level walking (LW) on a treadmill and four participants (TF02, TF04, TF05, and TF06) performed

a "ramp circuit." The treadmill protocol consisted of having users walk at six different steady-state speeds: 0.63, 0.72, 0.80, 0.89, 0.98, and 1.07 m/s, respectively. This range of speed was adjusted to ensure that all subjects were able to finish all the trials. Each subject walked for 1 minute in each of the six conditions. The ramp circuit involved starting in standing mode, taking a LW step(s), transitioning to RA, ascending a 5-m ramp, transitioning back to LW, transitioning to RD, descending a 5-m ramp, and finally transitioning back to LW. Five different presets were tested, the inclination angles were 7.8°, 9.2°, 11.0°, 12.4°, and 14.0°, respectively. An additional pilot study was conducted where one participant (TF02) was asked to walk with his respective passive leg (C-Leg with Triton Vertical Shock (VS) foot) in LW, and RA/descent at ±7.5° on a treadmill for 1 minute in each condition. VICON motion capture analysis was performed to generate the kinematics seen in both the knee and ankle joints of the passive leg.

Data Analysis

The investigators analyzed the biomechanics of walking using the outputs from sensors in the prosthesis. Each gait cycle was parsed using our finite-state machine with MATLAB. Ten gait cycles per participant and per condition were normalized to 100 data points to facilitate inter-subject comparisons. Outcome measures included joint kinematics and accuracy of the state machine in recognizing phase changes. A similar process was also performed for the ramp circuits by extracting out RA and RD gait cycles.

Joint kinematics were qualitatively compared to previously published results on people without amputation.[38,39] A repeated-measures analysis of variance was used to determine if there is a difference in the kinematic response between different walking speeds on the treadmill or incline/decline conditions on the ramp. Mauchly's Test of Sphericity tested variance across the conditions. When sphericity was violated, a Greenhouse–Geisser adjustment was applied. Kinematic outcome measures tested were peak knee flexion angle during swing, peak dorsiflexion angle in stance, and peak plantarflexion angle in push-off. To define the risk of type II error skewing the results due to the small sample size, observed power was calculated as $1-\beta$. An impedance parameter analysis was also performed to provide a recommended table of how the impedance parameters should be implemented across different ambulation modes.

RESULTS

Tuning Parameters

In LW, the three main parameters tuned included the ankle equilibrium angle in late stance, adjusting the transition threshold from early stance to late stance (T1) as well as from late stance to swing flexion (T2). In RA, only two unique parameters were adjusted that included the stiffness and damping of the knee joint in swing extension. In RD, two unique parameters, the stiffness, and damping in early stance were altered. Scaling equations (Eqs 2, 3, and 4) were utilized to adjust parameters with respect to kinematic and kinetic variables to ensure smoother gait.

The controller was able to robustly recognize the different phases of gait with no errors. The participants (TF01–TF03) took 265 strides, 265 strides, and 218 strides respectively during walking on the treadmill. This resulted in a total of 748 prosthesis steps that created 2992 phase transitions in the first experiment. In sloped walking, each individual took between 100 and 150 strides across all inclination angles resulting in a total of 839 steady-state prosthesis steps overall that produced a combined 3356 phases transitions during the ramp circuits. In total, there were 748 LW strides, 368 RA strides, and 471 RD strides with a total of 6348 phase transitions. In all cases, the state machine correctly recognized each part of the gait cycle (heel contact, mid-stance, toe-off, and early-to-mid swing) and altered joint impedance parameters accordingly. In terms of setting the transitional triggers, only two triggers required tuning during LW and these propagated to the ramp modes (Table 1).

Kinematics across Walking Speeds

The average knee angle remained extended during the stance portion of the gait phase (Fig. 3). Neither the knee flexion angle during swing($p = 0.349, 1 - \beta = 0.151$), the plantarflexion angle during push-off($p = 0.101, 1 - \beta = 0.412$), or the maximum dorsiflexion angle($p = 0.902, 1-\beta = 0.055$) changed as a function of walking speed on the treadmill. All subjects were able to walk at the range of 0.63–1.07 m/s on the treadmill without changing impedance parameters in the state machine.

Kinematics across Ambulation Modes

The impedance controller was able to generate walking gait that was comparable to able-bodied kinematics in many aspects but with a notable set of exceptions (Fig. 4). At the knee, the powered prosthesis did not provide stance phase knee flexion in any of the three modes but did allow for the user to have controlled knee flexion during RD. Swing phase closely matched able-bodied data in LW and RA, but additional swing flexion was not provided for RD. At the ankle, both controlled dorsiflexion and active powered plantarflexion were rendered during stance phase but were not as exaggerated in terms of ankle angle compared to the able-bodied subjects.

Kinematics across Inclination Angles

Both joint angles produced similar trajectories across inclination angles (Fig. 5). Neither the knee flexion angle during swing($p = 0.283, 1 - \beta = 0.213$), the plantar flexion angle during push-off($p = 0.337, 1 - \beta = 0.172$), or the maximum

TABLE 1. The final set of impedance parameters across participants for LW, RA, and RD

Mode	Phase	Ankle Parameters			Knee Parameters			Trigger Thresholds			
		k (Nm/deg)	b (Nms/deg)	θ (deg)	k (Nm/deg)	b (Nms/deg)	θ (deg)	T1 (deg)	T2 (% $F_{vertical}$)	T3 (deg/s)	T2 (% $F_{vertical}$)
Level Walking	*Early Stance*	EQ2	0.25	0	3	0.1	0	5.0 - 6.0	20.0 - 25.0	0.3	50
	Late Stance	EQ2	0.1	EQ3: p_{start} = 0 p_{final} = -17 to -23	EQ3: p_{start} = 3 p_{final} = 1	0.05	EQ3: p_{start} = 0 p_{final} = 63				
	Swing Flexion	2.6	0.1	1.75	1.4	0.1	63				
	Swing Extension	2.1	0.525	1.75	1.4	0.2	0				
Ramp Ascent	*Early Stance*	EQ2	0.25	0	3	0.15	0	6.5	Same as LW	0.4	50
	Late Stance	EQ2	0.1	Same as LW	EQ3: p_{start} = 3 p_{final} = 1	0.15	EQ3: p_{start} = 0 p_{final} = 63				
	Swing Flexion	2.6	0.1	1.75	1.4	0.1	63				
	Swing Extension	2.1	0.525	1.75	1.6 [1.4 to 2.0]	.20 [.15 to .25]	0				
Ramp Descent	*Early Stance*	3.5	0.25	0	2	.45 [.4 to .5]	EQ4 [.8 to .97]	Same as LW	Same as LW	0.3	40
	Late Stance	2.5	0.1	EQ3: p_{start} = 0 p_{final} = -11.5	EQ3: p_{start} = 2 p_{final} = 1	Previous Value	EQ3: p_{start} = Previous value p_{final} = 25				
	Swing Flexion	2.4	0.1	3	1.2	0.1	45				
	Swing Extension	2.4	0.1	3	2	0.15	0				

Note. Green highlights the subject-specific tuning parameters. Baseline values and the associated tuning range in brackets are displayed for each green highlight.

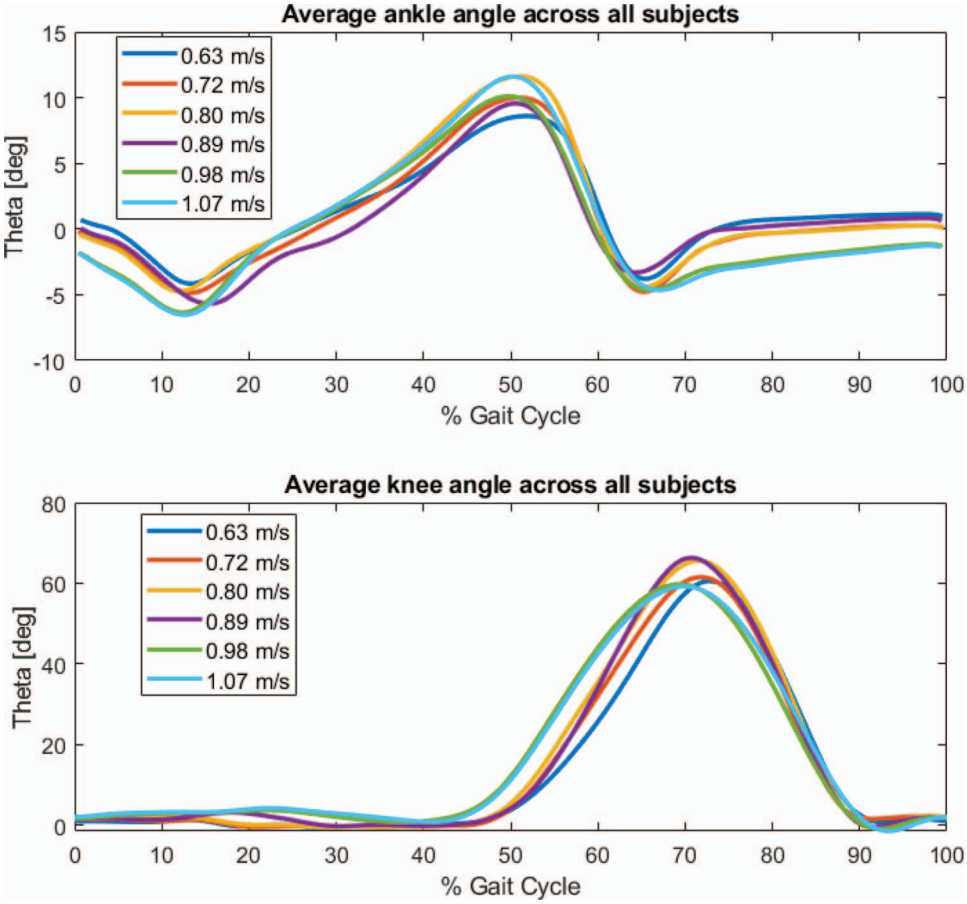

FIGURE 3. Average kinematic profiles of both ankle and knee joint during LW on a treadmill ($N = 3$) across different walking speeds.

dorsiflexion angle($p = 0.279, 1 - \beta = 0.201$) significantly changed as a function of ground incline angle on the ramp. All subjects were able to ascend the ramp between the range of 7.8° and 14.0° without changing impedance parameters in the RA mode.

Both joint angles produced similar trajectories across different decline angles (Fig. 6). Neither the knee flexion angle during swing ($p = 0.673, 1 - \beta = 0.084$), the plantarflexion angle during push-off ($p = 0.461, 1 - \beta = 0.106$), or the maximum dorsiflexion angle ($p = 0.3, 1 - \beta = 0.156$) significantly changed as a function of ground decline angle on the ramp. All subjects were able to descend the ramp between the range of 7.8–14.0° without changing impedance parameters in the RD mode.

DISCUSSION

In this study, the investigators developed a powered knee and ankle prosthesis with a controller that could recognize the different phases of gait, tune joint impedance across a range of gait speeds/inclination angles, and generate knee and ankle kinematics similar to individuals without amputation. The controller correctly recognized 6348 phase transitions across both walking speeds and inclination angles demonstrating the ability to render correct transitions to ensure reliable gait. The state machine's ability to correctly identify the phase of gait and set joint impedance parameters accordingly demonstrates its ability to assist users to ambulate over different conditions in a safe, seamless, and natural manner.

The tuning performed while the participant walked in the parallel bars was sufficient to obtain steady-state LW. There were seven unique parameters tuned across all ambulation modes (Table 1) that the investigators found useful for patient-specific accommodation. The final equilibrium angle of the ankle was tuned during late stance phase to improve push-off mechanics. There was some variance in the magnitude of tuned push-off preferred by the subjects, which was accommodated for using this parameter. The transition between early stance and late stance (T1) was tuned to ensure late stance was triggered by setting an ankle angle threshold. This setting was personalized for all subjects. The experimenters also found it useful to adjust the timing of the transition from late stance to swing flexion phase (T2). This parameter effectively controlled the speed of the swing-phase initiation.

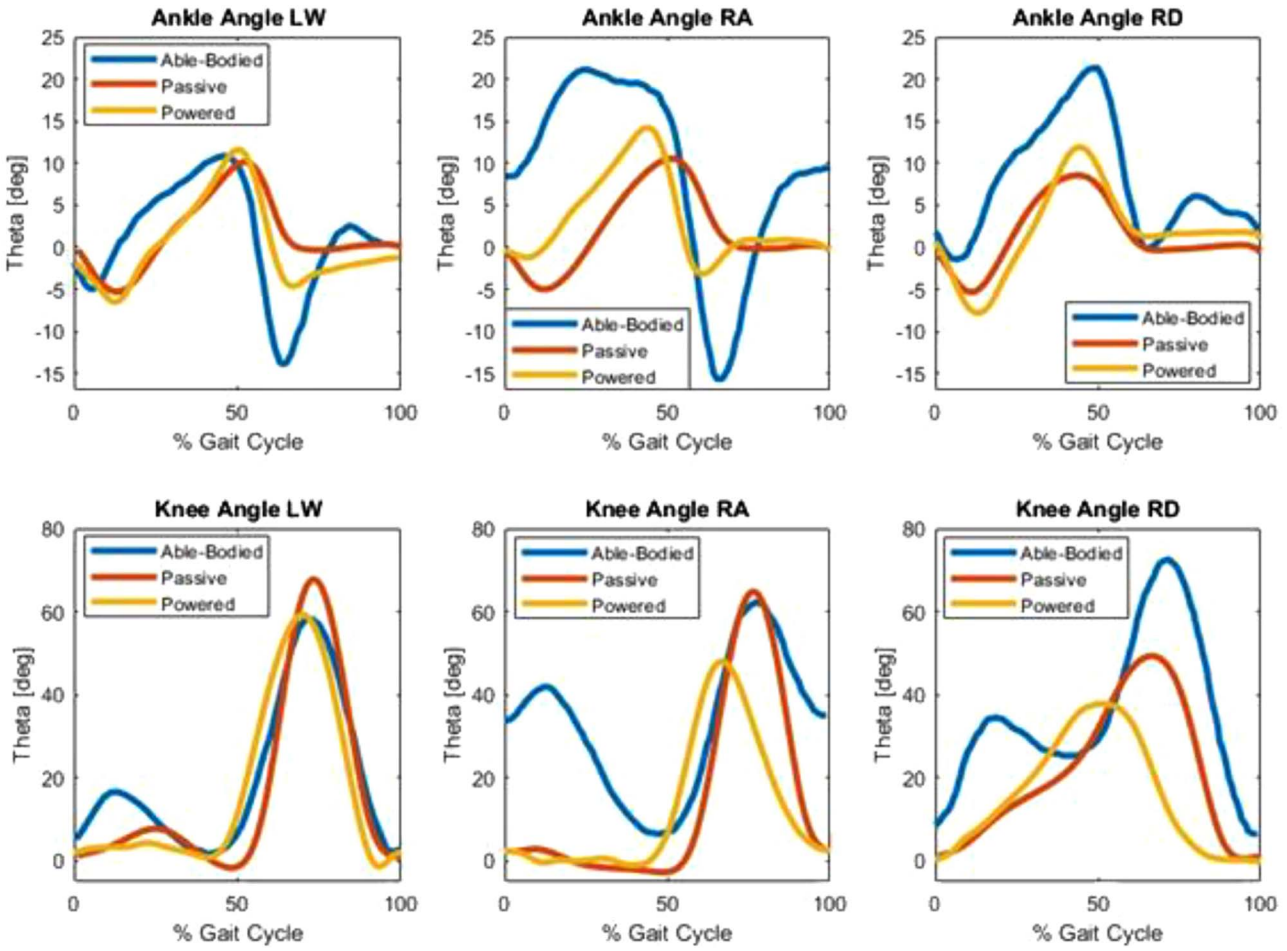

FIGURE 4. Kinematic profiles of both ankle and knee joint in 3 different ambulation modes: LW ($N = 3$), RA ($N = 4$), and RD ($N = 4$) comparing between healthy individuals ($N = 40$), and our powered prosthesis. Able-bodied LW and ramp kinematic profiles were found in previous literature.[38,39] Passive data is from a pilot study conducted for LW, RA/RD at $\pm 7.5°$.

In RA, the stiffness and damping were modified to control the acceleration of knee extension during the swing extension phase. In RD, two impedance parameters (knee damping and equilibrium angle) were tuned to maximize subject comfort. Of all the impedance parameters, the subject comfort was most sensitive to the RD settings during early stance phase at the knee.

Few parameters are necessary to clinically tune the prosthesis. This is in contrast to prior criticisms of impedance-based controllers.[21,23,40] This is likely due to the pairing of an impedance-based controller with a finite state machine, and the translatability of impedance settings seen in previous literature and used on a different prosthesis design.[8] This combination produced a fairly simple and intuitive methodology that enabled our clinicians to quickly tune the prosthesis and will facilitate future clinical translation. The tuning process may be improved further through integration with machine learning.

The lack of statistical differences across speeds or ramps for the kinematic variables were associated with low statistical power, indicating the sample size was insufficient to draw definitive conclusions how prosthetic knee and ankle kinematics vary on across speeds. Future research with more subjects may be able to better distinguish the finer details of how the prosthesis is performing across speeds. Therefore, this discussion will focus on the qualitative aspects of the knee and ankle kinematics compared to published data on people with intact limbs.

Knee and ankle kinematics closely followed able-bodied data during LW, regardless of speed, with a peak knee flexion angle of ~60° during swing flexion (Fig. 3). The initial knee flexion typically seen during able-bodied gait was not demonstrated in these subjects (Fig. 3). Initial knee flexion was induced during the tuning sessions; however, participants reported feeling less comfortable and would not tolerate this feature. Therefore, the knee flexion during early stance phase, normally seen in able-bodied gait (Figs 3 and 4), was tuned out of the device to maximize patient comfort as the device would be used in clinical practice. The subjects may not have preferred to have the knee flex during stance phase due to

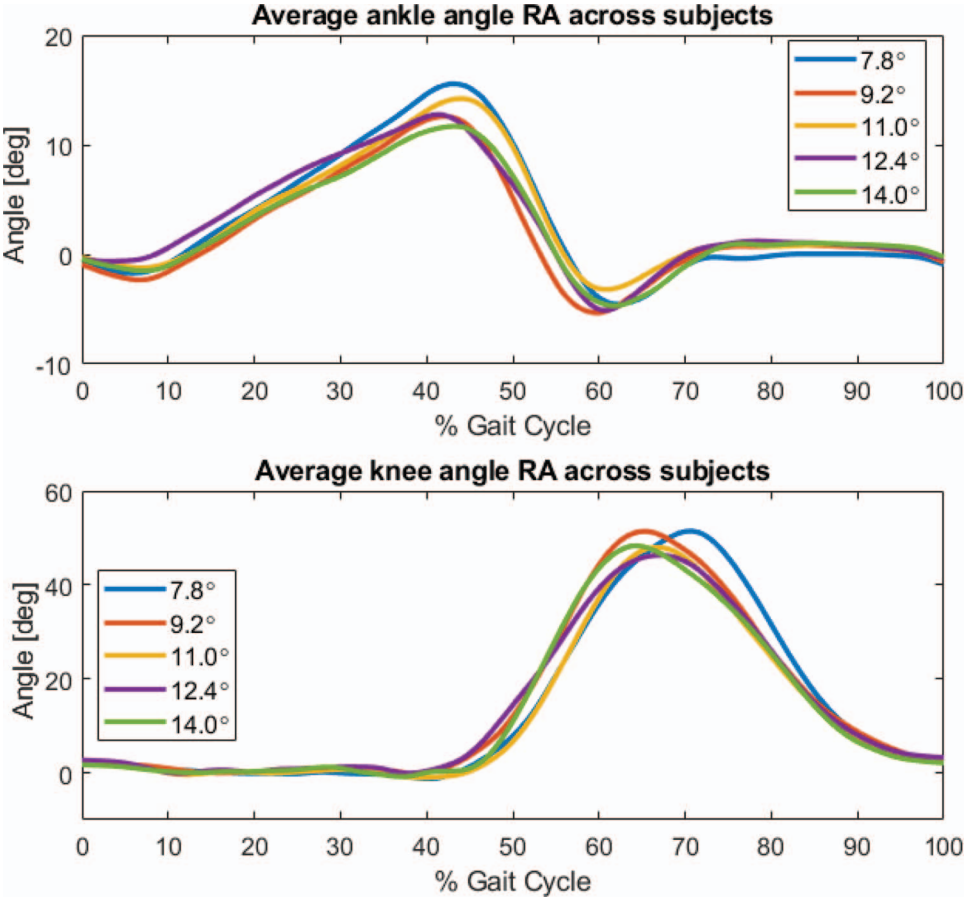

FIGURE 5. Average kinematic profiles of both ankle and knee joint in RA at five different inclination angles ($N = 4$).

motion inheritance in the limb/socket interface that would enable impact absorption to occur between the residual limb and the prosthetic socket, energy absorption normally handled by knee flexion. Alternatively, the users did not employ knee flexion strategies during stance in their own prostheses and, therefore, were not trained to use it in our prosthesis. Furthermore, the powered prosthesis exhibited powered ankle plantar flexion compared to the passive device during push-off in all ambulation modes, whereas the powered knee kinematics only matched in LW.

For RA, both the knee and ankle joints exhibited similar patterns across different inclination angles. For RD, the knee flexion tuning parameters were modulated based on user preference to ensure smooth transitions between stance and swing phase and allow the user to leverage the support provided by the high knee joint impedance and "ride" the prosthesis down during downhill walking. Future research, with more subjects, will be able to explore the details on how this controller is adapting to specific inclination angles.

Our study shows how our powered prosthesis is able to render similar kinematics to able-bodied individuals at normal and slow speeds but lacks the ability to compare to speeds in a higher range. For reference, healthy individuals' average preferred gait speed is approximately 1.4 m/s and transfemoral subjects' self-selected speed is approximately 1.2 m/s.[41,42] Even though our powered knee and ankle prosthesis provides more power compared to a passive prosthesis (Fig. 4), the increased mass and bulk compared to commercially available prostheses can still cause users to utilize their sound side more or use other compensatory movements when ambulating in different modes. As new technology emerges, weight and cost must be important considerations for building the future generation of robotic powered prostheses in order for them to be considered as viable options.

Future work that compares our powered knee-ankle prosthesis against the subject's personal passive prosthesis will allow us to understand the biomechanical differences between the sound versus the amputated side, and determine if common clinical outcome measures are met. Furthermore, a deeper understanding of how dual-powered prostheses compare against single-joint commercially available prostheses may be essential to disseminate this technology. This would allow us to understand whether there are differences between using two powered joints in synchrony versus putting two independently controlled powered joints "together."

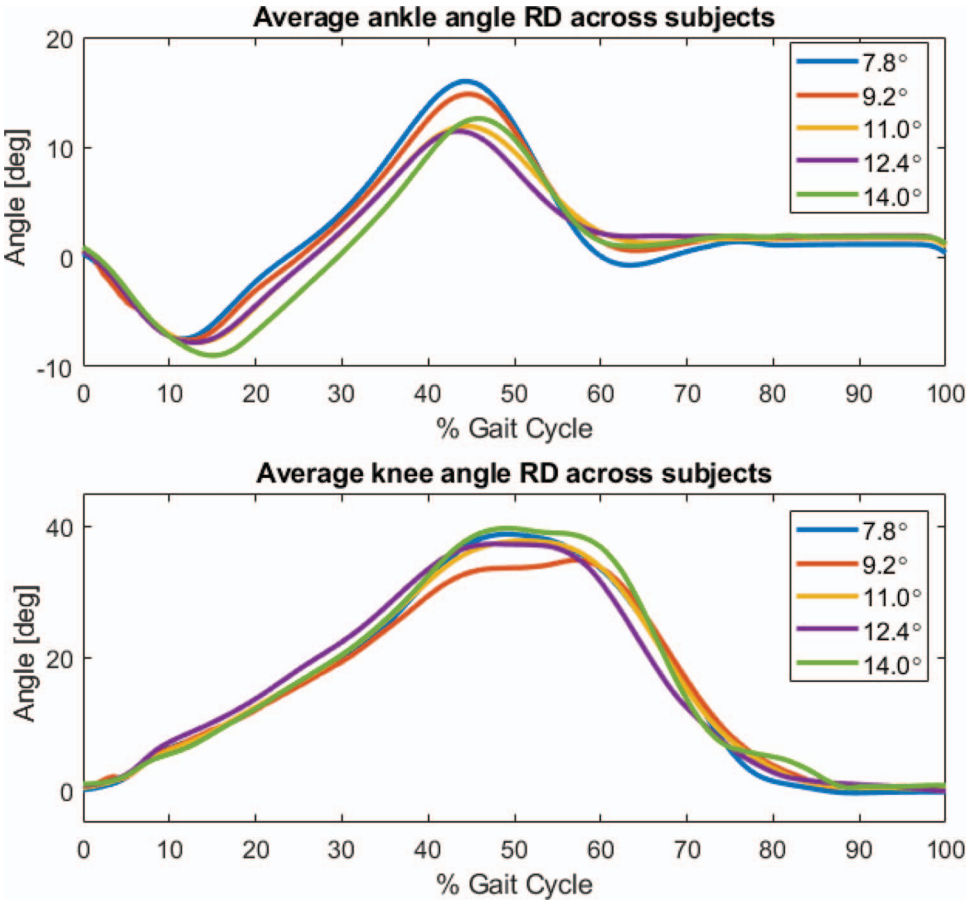

FIGURE 6. Average kinematic profiles of both ankle and knee joint in RD at five different inclination angles ($N = 4$).

CONCLUSION

This new powered knee and ankle prosthesis generated reliable walking gait across ambulation modes. The control system was able to correctly and robustly identify the phase of gait, set gait phase-specific impedance, and generate near-normal lower-limb kinematics using the minimal tuning of impedance parameters (7 out of 84). This controller was also capable of scaling powered assistance to the user across a range of walking speeds and inclination grades, which is a step toward being able to restore functionality lost through amputation.

SUPPLEMENTARY MATERIAL

Supplementary material is available at *MILMED* online.

ACKNOWLEDGMENTS

The authors acknowledge Aaron Ames and Eric Ambrose from the AMBER Lab at CalTech for their contributions on the mechanical design of the prosthetic device. The investigators thank Kinsey Herrin with the Georgia Tech MSPO program for patient fitting and guidance on device improvements as well as some undergraduate students (Jared Li, Alice Bok, and Noah Cho) who helped with data collection and analysis. The work was supported, in part, by a Fulbright fellowship awarded to Jonathan Camargo-Levya. I have obtained written permission from all persons named in the Acknowledgments.

FUNDING

This work was funded by Department of Defense Congressionally Directed Medical Research Programs (DoD CDMRP) Award No. W81XWH-17-1-0031. This work was supported by the Office of the Assistant Secretary of Defense for Health Affairs through the Orthotics and Prosthetics Outcomes Research Program Prosthetics Outcomes Research Award under Award No. W81XWH-17-1-0031.

REFERENCES

1. Ingraham KA, Fey NP, Simon AM, Hargrove JL: Assessing the relative contributions of active ankle and knee assistance to the walking mechanics of transfemoral amputees using a powered prosthesis. PLoS One; 2016; 11(1): e0147661.
2. Highsmith MJ, Goff LM, Lewandowski AL, et al: Low back pain in persons with lower extremity amputation: a systematic review of the literature. Spine J; 2019; 19(3): 552–63.
3. Bellmann M, Schmalz T, Blumentritt S: Comparative biomechanical analysis of current microprocessor-controlled prosthetic knee joints. Arch Phys Med Rehabil; 2010; 91(4): 644–52.
4. Thiele J, Westebbe B, Bellmann M, Kraft M: Designs and performance of microprocessor-controlled knee joints. Biomed Tech Eng; 2014; 59(1): 65–77.
5. Nolan L, Lees A: The functional demands on the intact limb during walking for active transfemoral and transtibial amputees. Prosthet Orthot Int; 2000; 24(2): 117–25.
6. Gailey R: Review of secondary physical conditions associated with lower-limb amputation and long-term prosthesis use. Artic J Rehabil Res Dev; 2008; 45(1): 15–30.

7. Morgenroth DC, Roland M, Pruziner AL, Czerniecki JM: Transfemoral amputee intact limb loading and compensatory gait mechanics during down slope ambulation and the effect of prosthetic knee mechanisms. Clin Biomech; 2018; 55: 65–72.
8. Simon AM, Ingraham KA, Fey NP, et al: Configuring a powered knee and ankle prosthesis for transfemoral amputees within five specific ambulation modes. PLoS One; 2014; 9(6): e99387.
9. Fey NP, Simon AM, Young AJ, Hargrove LJ: Controlling knee swing initiation and ankle plantarflexion with an active prosthesis on level and inclined surfaces at variable walking speeds. IEEE J Transl Eng Heal Med; 2014; 2: 1–12.
10. Young A, Simon A, Hargrove L: A training method for locomotion mode prediction using powered lower limb prostheses. IEEE Trans Neural Syst Rehabil Eng; 2014; 22(3): 671–7.
11. Rouse EJ, Mooney LM, Herr HM: Clutchable series-elastic actuator: implications for prosthetic knee design. Int J Rob Res; 2014; 33(13): 1611–25.
12. Hoover CD, Fulk GD, Fite KB: The design and initial experimental validation of an active myoelectric transfemoral prosthesis. J Med Device; 2012; 6(1): 011005.
13. Azocar AF, Member S, Mooney LM, Hargrove LJ, Rouse EJ: Design and characterization of an open-source robotic leg prosthesis. In: 2018 7th IEEE International Conference on Biomedical Robotics and Biomechatronics (Biorob); 2018:111-8.
14. Lawson BE, Mitchell J, Truex D, Shultz A, Ledoux E, Goldfarb M: A robotic leg prosthesis: design, control, and implementation. IEEE Robot Autom Mag; 2014; 21(4): 70–81.
15. Lambrecht BGA, Kazerooni H: Design of a semi-active knee prosthesis. In: 2009 IEEE International Conference on Robotics and Automation. IEEE; 2009: 639-45.
16. Lenzi T, Sensinger J, Lipsey J, Hargrove L, Kuiken T: Design and preliminary testing of the RIC hybrid knee prosthesis. In: 2015 37th Annual International Conference of the IEEE Engineering in Medicine and Biology Society. IEEE; 2015:1683-6.
17. Cempini M, Hargrove LJ, Lenzi T: Design, development, and bench-top testing of a powered polycentric ankle prosthesis. In: 2017 IEEE/RSJ International Conference on Intelligent Robots and Systems; 2017: 1064-9.
18. Jimenez-Fabian R, Verlinden O: Review of control algorithms for robotic ankle systems in lower-limb orthoses, prostheses, and exoskeletons. Med Eng Phys; 2012; 34(4): 397–408.
19. Goldfarb M, Lawson B, Shultz A: Realizing the promise of robotic leg prostheses. Sci Transl Med; 2013; 5(210):r 210ps15.
20. Varol HA, Sup F, Goldfarb M: Multiclass real-time intent recognition of a powered lower limb prosthesis. IEEE Trans Biomed Eng; 2010; 57(3): 542–51.
21. Gregg RD, Lenzi T, Hargrove LJ, Sensinger JW: Virtual constraint control of a powered prosthetic leg: from simulation to experiments with transfemoral amputees. IEEE Trans Robot; 2014; 30(6): 1455–71.
22. Holgate MA, Sugar TG, BÏohler AW: A novel control algorithm for wearable robotics using phase plane invariants. In: 2009 IEEE International Conference on Robotics and Automation. IEEE; 2009: 3845-50. Available at https://ieeexplore.ieee.org/abstract/document/5152565; accessed February 3, 2019.
23. Huang H, Crouch DL, Liu M, Sawicki GS, Wang D: A cyber expert system for auto-tuning powered prosthesis impedance control parameters. Ann Biomed Eng; 2016; 44(5): 1613–24.
24. Lenzi T, Hargrove LJ, Sensinger JW: Minimum jerk swing control allows variable cadence in powered transfemoral prostheses. In: 2014 36th Annual International Conference of the IEEE Engineering in Medicine and Biology Society. IEEE; 2014:2492-95. Available at https://ieeexplore.ieee.org/document/6944128; accessed February 13, 2019.
25. Quintero D, Villarreal DJ, Lambert DJ, Kapp S, Gregg RD: Continuous-phase control of a powered knee-ankle prosthesis: amputee experiments across speeds and inclines. IEEE Trans Robot; 2018; 1–16.
26. Ledoux ED, Goldfarb M: Control and evaluation of a powered transfemoral prosthesis for stair ascent. IEEE Trans Neural Syst Rehabil Eng; 2017; 25(7): 917–24.
27. Sup F, Bohara A, Goldfarb M: Design and control of a powered transfemoral prosthesis. Int J Rob Res; 2008; 27(2): 263–73.
28. Hogan: N: Impedance Control - an approach to manipulation part II - implementation. J. Dyn Syst Meas Control; 1985; 107(1): 1–7.
29. Shepherd MK, Rouse EJ: The VSPA foot: a quasi-passive ankle-foot prosthesis with continuously variable stiffness. IEEE Trans Neural Syst Rehabil Eng; 2017; 25(12): 2375–86.
30. Zhao H, Ambrose E, Ames AD: Preliminary results on energy efficient 3D prosthetic walking with a powered compliant transfemoral prosthesis. In: 2017 IEEE International Conference on Robotics and Automation; 2017:1140-7. Available at https://ieeexplore.ieee.org/document/7989136; accessed February 13, 2019.
31. Clauser CE, McConville JT, Young JW: Weight, volume, and center of mass of segments of the human body, 1969. https://apps.dtic.mil/dtic/tr/fulltext/u2/710622.pdf.
32. Young AJ, Simon AM, Fey NP, Hargrove LJ: Intent recognition in apowered lower limb prosthesis using time history information. Ann Biomed Eng; 2013; 42(3): 631–41.
33. Young AJ, Smith LH, Rouse EJ, Hargrove LJ: A comparison of the real-time controllability of pattern recognition to conventional myoelectric control for discrete and simultaneous movements. J Neuroeng Rehabil; 2014; 11: 5.
34. Spanias JA, Simon AM, Finucane SB, Perreault EJ, Hargrove LJ: Online adaptive neural control of a robotic lower limb prosthesis. J Neural Eng; 2018; 15(1): 016015.
35. Liu M, Zhang F, Datseris P, Huang H: Improving finite state impedance control of active-transfemoral prosthesis using dempster-shafer based state transition rules. J Intell Robot Syst Theory Appl; 2014; 76(3-4): 461–74.
36. Hogan N: Impedance control: an approach to manipulation: part II—implementation. J Dyn Syst Meas Control; 1985; 107(1): 8–16.
37. Rouse E, Hargrove L, Perreault E, Kuiken T: Estimation of Human Ankle Impedance During Walking Using the Perturberator Robot. In: Proceedings of the 4th IEEE RAS/EMBS International Conference on Biomedical Robotics and Biomechatronics. Rome, Italy; 2012. Available at https://ieeexplore.ieee.org/document/6290842; accessed February 13, 2019.
38. Kadaba MP, Ramakrishnan HK, Wootten ME: Measurement of lower extremity kinematics during level walking. J Orthop Res; 1990; 8(3): 383–92.
39. McIntosh AS, Beatty KT, Dwan LN, Vickers DR: Gait dynamics on an inclined walkway. J Biomech; 2006; 39(13): 2491–502.
40. Wen Y, Si J, Gao X, Huang S, Huang HH, Member S: A new powered lower limb prosthesis control framework based on adaptive dynamic programming. IEEE Trans Neural Networks Learn Syst; 2016: 1–6. Available at https://ieeexplore.ieee.org/document/7508991 accessed February 13, 2019.
41. Bohannon RW: Comfortable and maximum reference values and determinants. Age and comfortable and maximum walking speed of adults aged 20-79 years: reference values and determinants. Age and Ageing; 1997; 15–9.
42. Lamoth CJC, Ainsworth E, Polomski W, Houdijk H: Variability and stability analysis of walking of transfemoral amputees. Med Eng Phys; 2010; 1009–14.